

Superconductivity and Mössbauer effect of $\text{Fe}_x\text{Cu}_{1-x}\text{Ba}_2\text{YCu}_2\text{O}_{7+y}$ superconductors synthesized by high pressure

Y. H. Liu,* G. C. Che, K. Q. Li, and Z. X. Zhao

National Laboratory for Superconductivity, Institute of Physics, Chinese Academy of Sciences, P. O. Box 603, Beijing 100080, People's Republic of China

Z. Q. Kou, N. L. Di, and Z. H. Cheng

State Key Laboratory for Magnetism, Institute of Physics, Chinese Academy of Sciences, P. O. Box 603, Beijing 100080, People's Republic of China

(Received 7 July 2004; revised manuscript received 6 December 2004; published 7 March 2005)

The superconductivity in $\text{Fe}_x\text{Cu}_{1-x}\text{Ba}_2\text{YCu}_2\text{O}_{7+y}$ superconductors ($0.00 \leq x \leq 0.70$) is improved by high-pressure (HP) synthesis. The HP samples have higher oxygen content than the ambient pressure (AM) samples. Mössbauer effect studies confirmed that the high-pressure synthesis changes the local structure on the atomic scale. For the HP samples Fe (2) in the CuO_2 planes has highly symmetric pyramidal-oxygen coordination. The tetragonal coordinated Fe (1) in the CuO_x chains disappears and becomes the one having fivefold and sixfold oxygen coordination after the high-pressure synthesis. This suggests that the increase of oxygen content and the change of local structure are important reasons for the improvement of superconductivity in the HP samples.

DOI: 10.1103/PhysRevB.71.104503

PACS number(s): 74.62.Bf, 74.62.Dh, 76.80.+y

I. INTRODUCTION

Studies on transition-metal substitution have enhanced our understanding of the superconducting and normal-state properties of high- T_c superconductors. Substitutions of metals for Cu in $\text{YBa}_2\text{Cu}_3\text{O}_{7-y}$ (YBCO) usually depress T_c . Among all the transition elements, divalent ions Zn^{2+} and Ni^{2+} substitute for Cu (2) located in CuO_2 planes¹⁻⁴ and the trivalent ion Co^{3+} occupies Cu (1) sites located in CuO_x chains. It is very interesting that the trivalent ion Fe^{3+} with magnetism enters into both CuO_2 planes and CuO_x chains in the $\text{Fe}_x\text{Cu}_{1-x}\text{Ba}_2\text{YCu}_2\text{O}_{7+y}$ system.⁵⁻⁷ The T_c decreases with increasing Fe content and becomes zero when x exceeds 0.3.^{8,9} Furthermore, Fe content in CuO_2 planes increases with increasing Fe dopant⁶ and an orthorhombic-to-tetragonal structural transition takes place at $x \geq 0.1$.^{5,8,9} Another interesting aspect is that substitution of Fe for Cu is helpful to study the local magnetism and structure using Mössbauer technique.¹⁰

The interplay between magnetism and superconductivity was investigated at all times to understand better the origin of the superconductivity. Recently, the coexistence of superconductivity and ferromagnetism was discovered in $R_{2-x}\text{Ce}_x\text{RuSr}_2\text{Cu}_2\text{O}_{10}$ ($R=\text{Eu}$ and Gd , $x=0.4$ and 0.6)^{11,12} and $\text{RuSr}_2\text{RCu}_2\text{O}_8$, with $R=\text{Y}$ and Gd (Ru-1212 type), high- T_c superconductors.^{13,14} Because Fe and Ru have similar chemical properties, it is expected that the cuprate superconductors containing high Fe content will provide more information on the interplay between magnetism and superconductivity.

At early stage of studies on high- T_c superconductors, several groups reported superconductivity in $\text{YSr}_2\text{Cu}_{2-x}\text{Fe}_x\text{O}_{7+y}$ system with $x \geq 0.3$ prepared in high-pressure oxygen^{15,16} and Ca-doped $\text{YSr}_2\text{Cu}_{2.5}\text{Fe}_{0.5}\text{O}_{7+y}$ system.¹⁷ Subsequently, Shi *et al.* improved superconductivity in $\text{YSr}_2\text{Cu}_{2.7}\text{Fe}_{0.3}\text{O}_{7+y}$ by high-pressure oxygen (27 MPa) annealing and enhanced T_c up to 60 K.¹⁸ Recently, the $\text{FeSr}_2\text{YCu}_2\text{O}_{7+y}$ supercon-

ductor was obtained and the crystal structure and superconductivity were systematically investigated.^{19,20}

Very recently, we investigated the influence of preparation conditions on the lattice parameters and superconductivity of $\text{Fe}_{0.5}\text{Cu}_{0.5}\text{Ba}_2\text{YCu}_2\text{O}_{7+y}$ in a previous paper²¹ and prepared $\text{Fe}_{0.5}\text{Cu}_{0.5}(\text{Ba}_{1-x}\text{Sr}_x)_2\text{YCu}_2\text{O}_{7+y}$ superconductors with $x=0, 0.5$, and 1.0 using the high-pressure technique.²²

In this paper, comprehensive studies of x-ray diffraction, oxygen content, superconductivity, annealing, and Mössbauer spectroscopy on the $\text{Fe}_x\text{Cu}_{1-x}\text{Ba}_2\text{YCu}_2\text{O}_{7+y}$ system prepared by the high-pressure synthesis are presented to help one understand the Fe-doped YBCO.

II. EXPERIMENTAL PROCEDURE AND RESULTS

A. Sample preparation

$\text{Fe}_x\text{Cu}_{1-x}\text{Ba}_2\text{YCu}_2\text{O}_{7+y}$ samples ($0.00 \leq x \leq 0.80$) were prepared in two steps. In the first step, the starting materials, high-purity (99.99%) powders of Y_2O_3 , BaCO_3 , CuO , and Fe_2O_3 according to the formula of $\text{Fe}_x\text{Cu}_{1-x}\text{Ba}_2\text{YCu}_2\text{O}_{7+y}$ ($x=0.00, 0.06, 0.10, 0.16, 0.32, 0.40, 0.50, 0.60, 0.70, 0.80$) were thoroughly mixed in a mortar. The mixtures were heated in air in the temperature range $880^\circ\text{C} \leq T \leq 930^\circ\text{C}$ for at least 70 h with intermediate grindings. Then, the mixtures were reground and pressed into pellets, which were sintered at 930°C for 40 h in air and cooled down to room temperature at a rate of 30°C per hour. The resultant ambient pressure samples were named AM samples. In the second step, the AM samples were powdered, mixed with 5 wt % KClO_4 powder and pressed into pellets with diameter of 7 mm and thickness of 5 mm, which were wrapped in gold foil and synthesized at 1000°C under high pressure of 6 GPa for 0.5 h in a belt-type apparatus. The sample chamber of the belt-type apparatus used pyrophyllite as the pressure-transmitting medium and a graphite tube as an in-

ternal heater. The synthesis temperature was controlled by the electrical input power imposed on the graphite sleeve. The resultant products were quenched from 1000 °C to room temperature by shutting off the electrical power before releasing the pressure. These products were named HP samples.

B. Sample characterization

Both the AM and HP samples were characterized by powder XRD using a MXP18A-HF type diffractometer with $\text{CuK}\alpha$ radiation.

The POWDERX program²³ was used to determine the lattice parameters. The results indicate that all the AM and HP samples of $\text{Fe}_x\text{Cu}_{1-x}\text{Ba}_2\text{YCu}_2\text{O}_{7+y}$ are of single phase except for the samples with $x=0.80$ and the solid solubility limit of Fe in the $\text{Fe}_x\text{Cu}_{1-x}\text{Ba}_2\text{YCu}_2\text{O}_{7+y}$ system is about 0.80, which is consistent with the results of Tarascon *et al.*⁸ From the dependence of lattice parameters on Fe content as shown in Fig. 1, it is found that the AM samples become tetragonal at $x \geq 0.10$, which is consistent with previous reports on the Fe-doped YBCO.^{5,8,9} The HP samples have smaller lattice parameter c and unit-cell volume than the AM samples, which is related to the increase of oxygen content in the HP samples due to the high-pressure synthesis. This phenomenon has been observed in YBCO synthesized in air²⁴ or in the high-pressure oxygen²⁵ and in Fe-doped $\text{YSr}_2\text{Cu}_3\text{O}_{7-y}$ synthesized in high-pressure oxygen.^{18,20}

Figure 2 shows the typical XRD patterns of AM-(a) and HP-(b) samples of $\text{Fe}_{0.5}\text{Cu}_{0.5}\text{Ba}_2\text{YCu}_2\text{O}_{7+y}$.²¹ Structural analysis indicates that they have tetragonal structure belonging to space group $P4/mmm$. The lattice parameters of AM and HP samples are $a=0.3874$, $c=1.167$ nm and $a=0.3865$, $c=1.1598$ nm, respectively.

C. Measurements of oxygen content

The oxygen contents of the AM and HP samples were measured using iodometric titration.²⁷ It must be pointed out that there was a small amount of KCl and KClO_4 in the HP samples due to the addition of KClO_4 used as an oxidant and the incomplete decomposition during the high-pressure synthesis. To minimize its influence on the titration results, the bulk HP samples were powdered, washed using distilled water and dried below 80 °C before determining the oxygen content. The purified powder was still superconducting as checked by magnetization measurements. The results of iodometric titration indicate that the oxygen contents in both the AM and HP samples increase with increasing Fe content, as shown in Fig. 3. Also one can find that the HP-samples have higher oxygen content than the AM samples. The oxygen content in the AM samples is well consistent with those reported in Refs. 8, 24, and 27.

D. Superconductivity

dc magnetic measurements were performed using a SQUID magnetometer (Quantum Design, MPMS type). Figure 4 shows $M-T$ curves of the AM-(a) and HP-(b) samples. The dependence of T_c on Fe content for the HP and AM

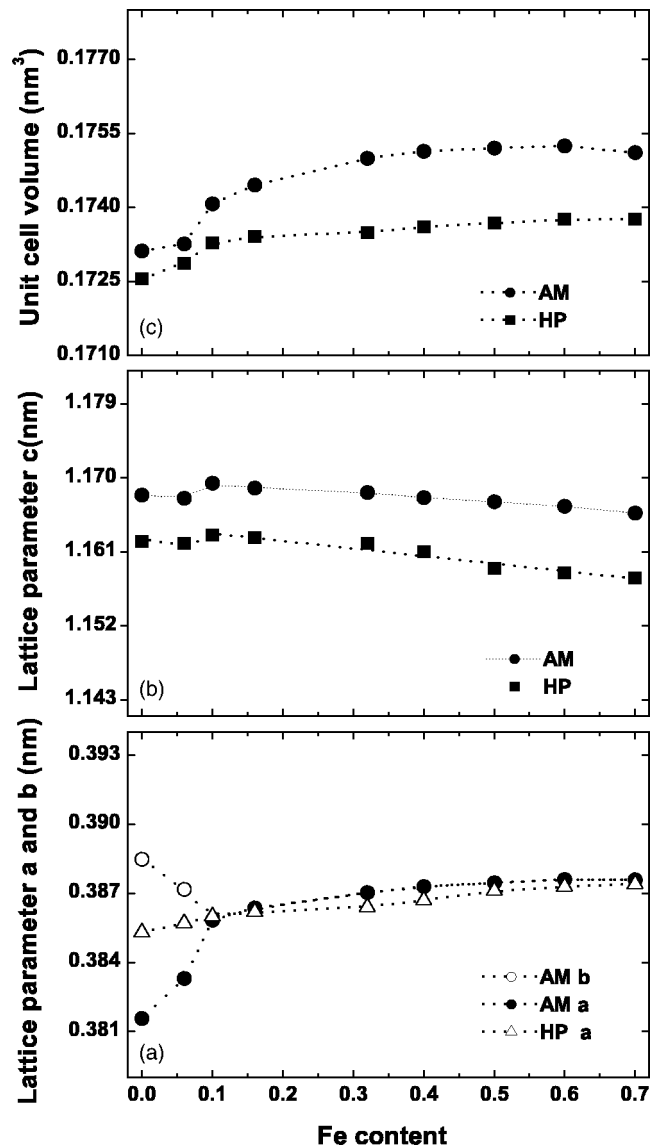


FIG. 1. The dependence of lattice parameters a , b (A) and c (B) and unit-cell volume (C) of the AM and HP samples of $\text{Fe}_x\text{Cu}_{1-x}\text{Ba}_2\text{YCu}_2\text{O}_{7+y}$ on Fe content.

samples is shown in Fig. 5. It can be seen that for the AM samples T_c decreases quickly with increasing Fe content and becomes zero at $x=0.4$, which is in agreement with the results of Tarascon *et al.*⁸ For the HP samples, however, with increasing Fe content the decrease of T_c is very slow, indicating that the high-pressure synthesis improves superconductivity.

Figure 6 shows the $R-T$ and $M-T$ curves of the AM and HP samples of $\text{Fe}_{0.5}\text{Cu}_{0.5}\text{Ba}_2\text{YCu}_2\text{O}_{7+y}$. These results indicate that the HP sample has a superconducting transition temperature $T_c=80$ K. The shielding and Meissner fraction is about 50 and 24 %, respectively, indicating that the HP sample with $x=0.50$ has bulk superconductivity. The AM sample has a semiconductorlike behavior in the $R-T$ curve, even after oxygenation at 350 °C for 40 h in flowing oxygen under ambient pressure.

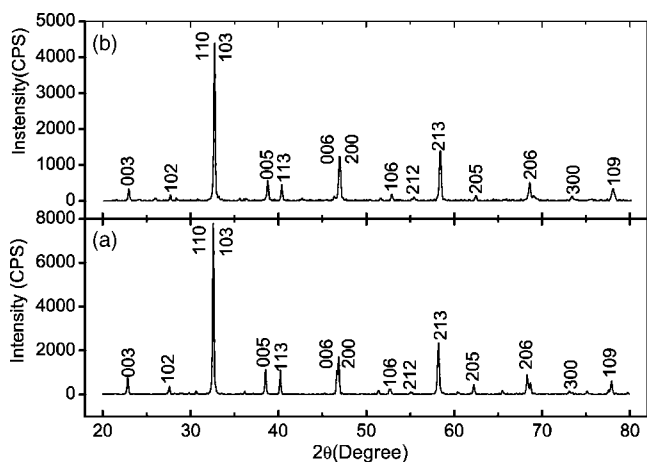


FIG. 2. XRD patterns of the AM sample (a) and HP sample (b) of $\text{Fe}_{0.5}\text{Cu}_{0.5}\text{Ba}_2\text{YCu}_2\text{O}_{7+y}$ compound.

E. Annealing experiments

In order to know the stability of oxygen absorbed (HPO) in the lattice due to the high-pressure synthesis and find out the possible reasons for the improvement of superconductivity, two HP samples were selected for annealing experiments at different temperatures.

Two typical HP samples (A) $\text{Fe}_{0.06}\text{Cu}_{0.94}\text{Ba}_2\text{YCu}_2\text{O}_{7.25}$ and (B) $\text{Fe}_{0.5}\text{Cu}_{0.5}\text{Ba}_2\text{YCu}_2\text{O}_{7.41}$ were annealed at 150, 250, 350, 450, 650, and 900 °C for 2 h in air and then quenched to room temperature. The reasons for selecting these two HP samples are that the AM samples of the HP samples (A) and (B) have orthorhombic and tetragonal structure, respectively. On the other hand, the AM sample of (A) is superconducting and that of (B) is an insulator. It is advantageous to distinguish the influence of HPO on structure and superconductivity of samples during the annealing process. Figures 7(a) and 7(b) show the influence of the annealing temperature (T_a) on the $M-T$ curves of the annealed HP samples (A) and (B),

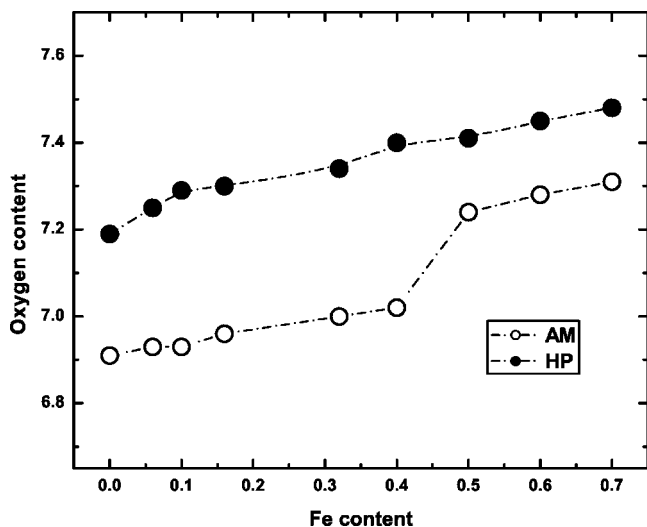


FIG. 3. The dependence of oxygen content on Fe content for the AM and HP samples of $\text{Fe}_x\text{Cu}_{1-x}\text{Ba}_2\text{YCu}_2\text{O}_{7+y}$. The limit of measurement error is less than 0.02.

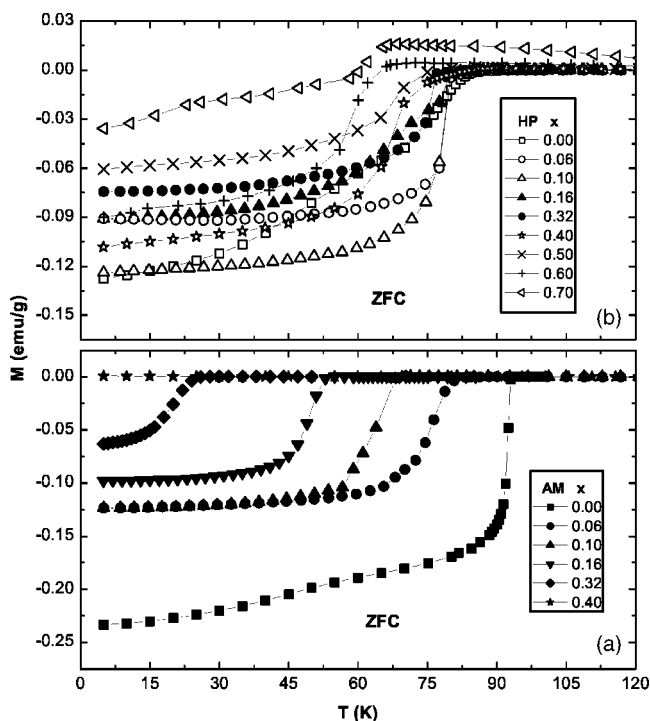


FIG. 4. The $M-T$ curves of the AM (a) and HP (b) samples of $\text{Fe}_x\text{Cu}_{1-x}\text{Ba}_2\text{YCu}_2\text{O}_{7+y}$.

respectively. Results indicate that the T_c of HP sample (B) gradually decreases with increasing T_a and becomes zero at $T_a \geq 450$ °C. For the HP sample (A), T_c is constant in the annealing temperature range of 150–350 °C, then at 450 °C decreases to 85 K which is as high as T_c of its AM sample (see Fig. 8).

On the other hand, the lattice parameters of the two annealed HP samples have also changed regularly with increasing T_a . Figure 9 shows the influence of T_a on the local XRD patterns ($46^\circ \leq 2\theta \leq 48^\circ$) of the two annealed HP samples.

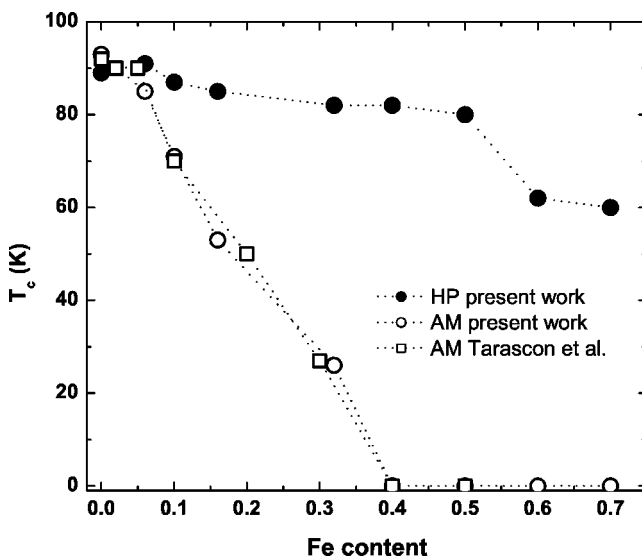


FIG. 5. The dependence of T_c on Fe content for the AM and HP samples of $\text{Fe}_x\text{Cu}_{1-x}\text{Ba}_2\text{YCu}_2\text{O}_{7+y}$.

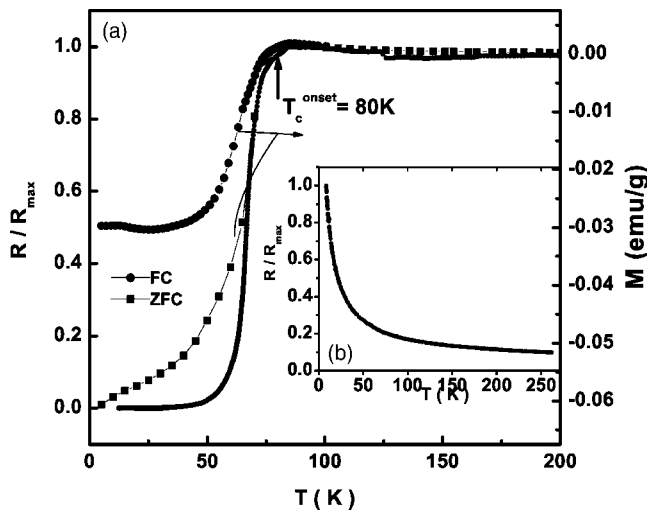


FIG. 6. (a) ZFC and FC M - T curves and R - T curve of the HP sample of $\text{Fe}_{0.5}\text{Cu}_{0.5}\text{Ba}_2\text{YCu}_2\text{O}_{7+x}$. (b) R - T curve of the AM sample of $\text{Fe}_{0.5}\text{Cu}_{0.5}\text{Ba}_2\text{YCu}_2\text{O}_{7+x}$.

The dependence of lattice parameters a , b , and c on T_a is shown in Fig. 10. For the HP sample (A), the shift of the diffraction peak of (006) to lower angle is not obvious at $150^\circ\text{C} \leq T_a \leq 350^\circ\text{C}$. For $T_a \geq 350^\circ\text{C}$, the peak of (006) gradually shifts to lower angle and the peaks of (002) and

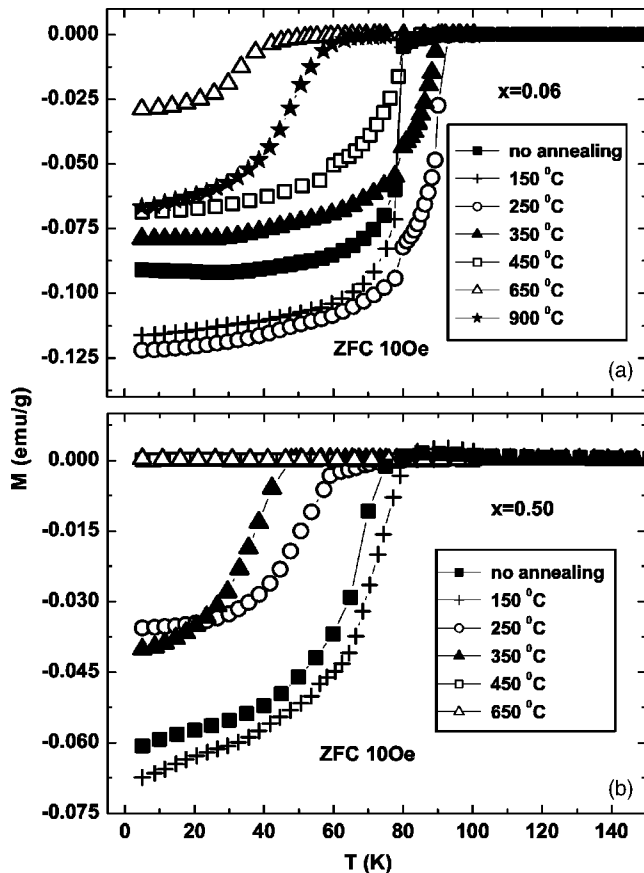


FIG. 7. The influence of annealing temperature T_a on the M - T curves of HP samples (A) $\text{Fe}_{0.06}\text{Cu}_{0.094}\text{Ba}_2\text{YCu}_2\text{O}_{7.25}$ (a) and (B) $\text{Fe}_{0.5}\text{Cu}_{0.5}\text{Ba}_2\text{YCu}_2\text{O}_{7.41}$ (b).

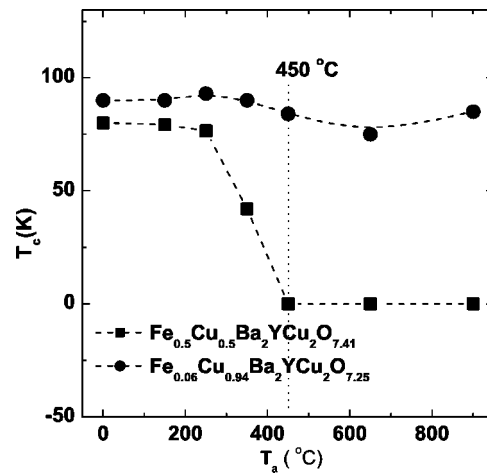


FIG. 8. The dependence of T_c on T_a for the HP samples (A) $\text{Fe}_{0.06}\text{Cu}_{0.094}\text{Ba}_2\text{YCu}_2\text{O}_{7.25}$ and (B) $\text{Fe}_{0.5}\text{Cu}_{0.5}\text{Ba}_2\text{YCu}_2\text{O}_{7.41}$.

(200) become apparent. This means that lattice parameter c increases gradually and the HP sample (A) undergoes a tetragonal-orthorhombic structural transition during the annealing process, which can be found in Fig. 9(a). For the HP sample (B), the peak of (006) shifts to lower angle with increasing T_a [see Fig. 9(b)], indicating that lattice parameter c increases with increasing T_a , as shown in Fig. 10(b). It is well known that in the pure YBCO system, the length of lattice parameter c is inversely proportional to the oxygen content. The more oxygen content the samples have, the shorter the lattice parameter c becomes. Based on this and the change of lattice parameter c during the whole annealing process, it is speculated that with increasing annealing temperature the oxygen content of the HP samples (A) and (B) is gradually released. The release of HPO results in the absence of superconductivity in the HP sample (B) and a decrease of T_c in HP sample (A) at $T_a = 450^\circ\text{C}$. From these observa-

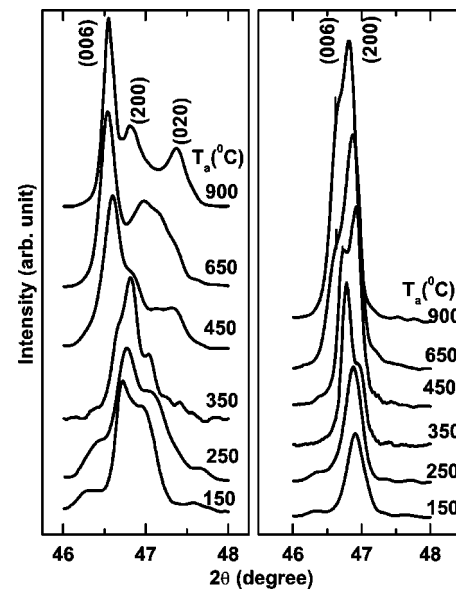


FIG. 9. The evolution of local XRD patterns ($46^\circ \leq 2\theta \leq 48^\circ$) of (a) $\text{Fe}_{0.06}\text{Cu}_{0.094}\text{Ba}_2\text{YCu}_2\text{O}_{7.25}$ and (b) $\text{Fe}_{0.5}\text{Cu}_{0.5}\text{Ba}_2\text{YCu}_2\text{O}_{7.41}$.

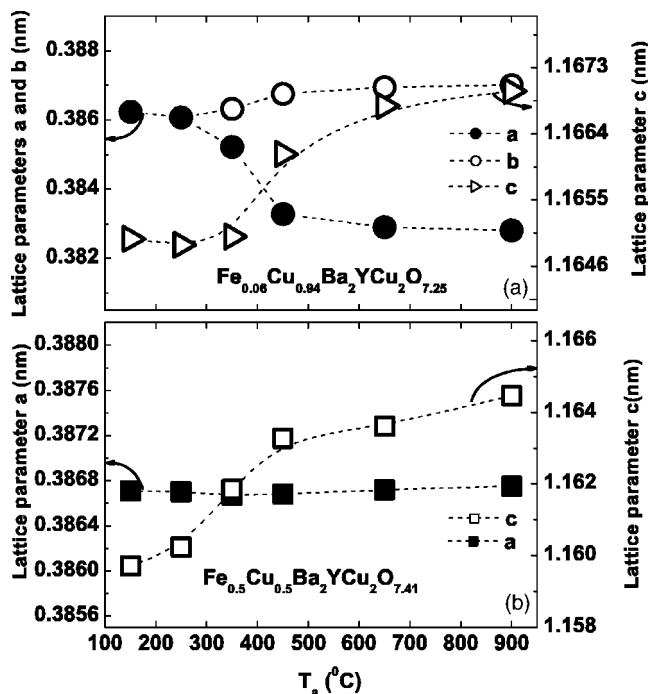


FIG. 10. The dependence of lattice parameters a , b (a) and c (b) of the HP samples (A) $\text{Fe}_{0.06}\text{Cu}_{0.84}\text{Ba}_2\text{YCu}_2\text{O}_{7.25}$ and (B) $\text{Fe}_{0.5}\text{Cu}_{0.5}\text{Ba}_2\text{YCu}_2\text{O}_{7.41}$ on T_a .

tions, we suggest that the HPO plays an important role in the improvement of superconductivity in the HP samples. The annealing experiments also indicate that the HPO is different from the oxygen entering the lattice in air under ambient pressure. The latter enters the lattice at 350–500 °C.²⁴

F. Mössbauer effect

The Mössbauer technique has been shown^{5–7,16–18} to be a powerful tool determining the distribution of Fe between Cu (1) and Cu (2) sites. In order to obtain information on the distribution of Fe between the Cu (1) and Cu (2) sites in the AM and HP samples and to further find out the reasons for the improvement of superconductivity in the HP samples, five samples with different Fe content, one AM sample $\text{Fe}_{0.5}\text{Cu}_{0.5}\text{Ba}_2\text{YCu}_2\text{O}_{7.24}$ and four HP samples $\text{Fe}_{0.16}\text{Cu}_{0.84}\text{Ba}_2\text{YCu}_2\text{O}_{7.30}$, $\text{Fe}_{0.32}\text{Cu}_{0.68}\text{Ba}_2\text{YCu}_2\text{O}_{7.34}$, $\text{Fe}_{0.04}\text{Cu}_{0.6}\text{Ba}_2\text{YCu}_2\text{O}_{7.40}$, and $\text{Fe}_{0.5}\text{Cu}_{0.5}\text{Ba}_2\text{YCu}_2\text{O}_{7.41}$, were selected for Mössbauer effect studies.

⁵⁷Fe Mössbauer spectra of samples were recorded by a Wissel System constant acceleration Mössbauer spectrometer with ⁵⁷Co (Pd) source at room temperature. The velocity was calibrated using α -Fe foil. The values of isomer shift given here were relative to α -Fe at room temperature. A least-squares program was used to fit the spectra with Lorentzian line shapes.

Figures 11 and 12 show the results of Mössbauer effect of the selected AM and HP samples. The spectra can be best fit to four subspectra (A, B, C, and D). The hyperfine parameters of isomer shift (δ), quadrupole splittings (Δ), full-width-at-half-maximum (FWHM) (Γ), and site intensity ratio (I_n/I) of these four subspectra are summarized in Table I. A

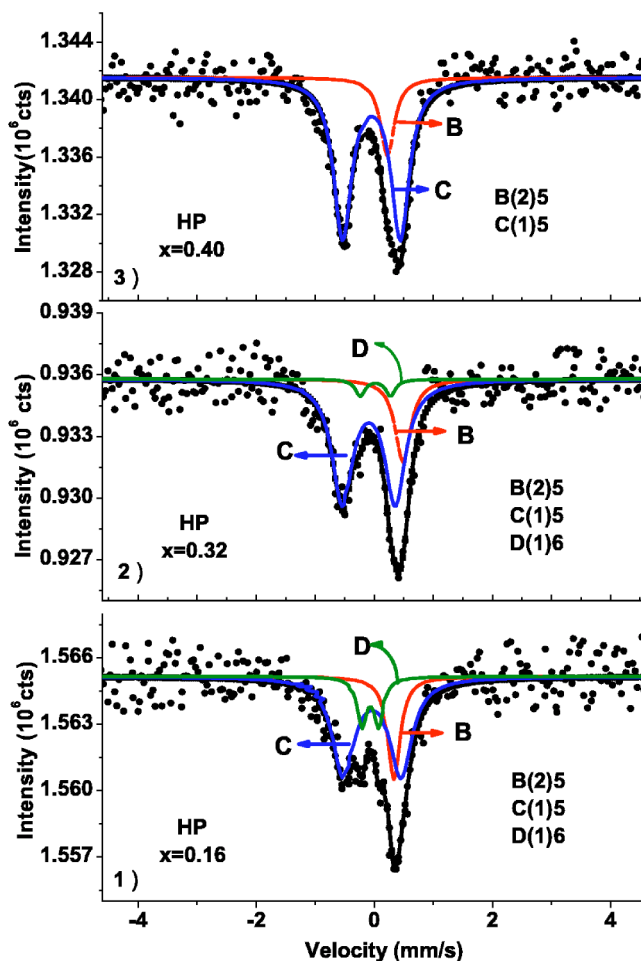


FIG. 11. (Color online) Room-temperature Mössbauer spectra of the HP samples (1) $\text{Fe}_{0.16}\text{Cu}_{0.84}\text{Ba}_2\text{YCu}_2\text{O}_{7.30}$, (2) $\text{Fe}_{0.32}\text{Cu}_{0.68}\text{Ba}_2\text{YCu}_2\text{O}_{7.34}$, and (3) $\text{Fe}_{0.4}\text{Cu}_{0.6}\text{Ba}_2\text{YCu}_2\text{O}_{7.40}$. The notation (i) n denotes that the Fe occupies Cu(i) site and has n -fold oxygen coordination.

consensus that doublets A, C, and D are ascribed to the Fe located at Cu (1) sites and subspectrum B is related to the Fe located at Cu (2) sites has been obtained.^{5,17,18,29} Moreover, the Fe atoms corresponding to doublets A, C, and D have tetragonal, fivefold, and sixfold oxygen coordination,^{5,18,29} respectively, and the Fe corresponding to subspectrum B has the same pyramidal configuration of oxygen as Cu (2).^{5,17,18,29}

Figures 11(1), 11(2) and 11(3) show the Mössbauer spectra of the HP samples (1) $\text{Fe}_{0.16}\text{Cu}_{0.84}\text{Ba}_2\text{YCu}_2\text{O}_{7.30}$, (2) $\text{Fe}_{0.32}\text{Cu}_{0.68}\text{Ba}_2\text{YCu}_2\text{O}_{7.34}$, and (3) $\text{Fe}_{0.4}\text{Cu}_{0.6}\text{Ba}_2\text{YCu}_2\text{O}_{7.40}$, respectively. From the three figures, two main features can be observed. One is that the subspectrum B of the HP samples with $x \leq 0.40$ is a singlet splitting while subspectrum B is a doublet splitting of the HP sample with $x=0.50$ [see Fig. 12(2)]. The singlet splitting implies that the oxygen environment about the Fe located in CuO_2 planes is highly symmetric. The other main feature is that the Mössbauer spectra of HP samples with $x=0.16$ and 0.32 can be fit well according to three subspectra and doublet D is attributed to the sixfold coordinated Fe in CuO_x chains.²⁹

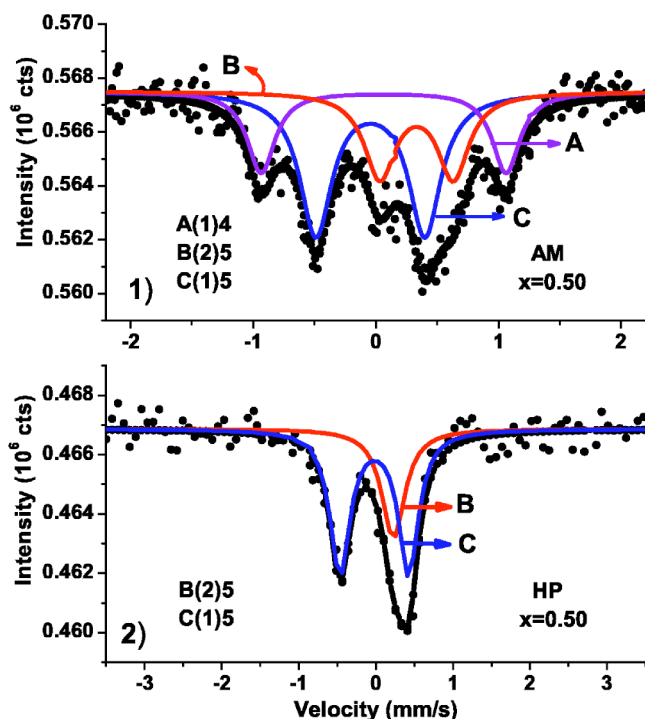


FIG. 12. (Color online) Room-temperature Mössbauer spectra of the samples (1) the AM sample, $\text{Fe}_{0.5}\text{Cu}_{0.5}\text{Ba}_2\text{YCu}_2\text{O}_{7.24}$ and (2) the HP sample $\text{Fe}_{0.5}\text{Cu}_{0.5}\text{Ba}_2\text{YCu}_2\text{O}_{7.41}$. The notation $(i)n$ denotes that the Fe occupies Cu(i) site and has n -fold oxygen coordination.

In order to obviously observe the changes in the local oxygen environment about Fe after the high-pressure synthesis, a comparison between the Mössbauer spectra of the HP samples with $x=0.50$ and that of its AM sample is indispensable (see Fig. 12). One can find that the doublet C increases at the expense of the doublet A in going from the AM sample to the HP sample and the doublet A disappears in the spectra

TABLE I. Room-temperature Mössbauer effect parameters: δ -isomer shift (relative to α -Fe at room temperature), Δ -quadrupole splitting, Γ -FWHM, I_n/I -site intensity ratio for the AM and HP samples of $\text{Fe}_x\text{Cu}_{1-x}\text{Ba}_2\text{YCu}_2\text{O}_{7+y}$.

Sample	x	Site	δ (mm/s)	Δ (mm/s)	Γ (mm/s)	I_n/I
HP	0.16	B:	0.334(6)		0.131(1)	0.20(1)
		C:	-0.034(6)	0.972(0)	0.221(0)	0.66(3)
		D:	-0.064(8)	0.281(4)	0.101(3)	0.14(2)
HP	0.32	B:	0.487(8)		0.161(9)	0.19(8)
		C:	-0.091(5)	0.90(1)	0.211(6)	0.76(2)
		D:	0.02(2)	0.51(3)	0.100(3)	0.050(2)
HP	0.40	B:	0.224(4)		0.145(6)	0.16(6)
		C:	-0.046(2)	0.977(3)	0.183(2)	0.84(9)
HP	0.50	B:	0.213(4)	0.163(7)	0.097(0)	0.24(1)
		C:	-0.015(3)	0.889(4)	0.161(4)	0.76(0)
AM	0.50	A:	0.062(2)	1.996(4)	0.136(4)	0.23(8)
		B:	0.331(3)	0.599(4)	0.154(4)	0.28(0)
		C:	-0.045(1)	0.889(3)	0.159(3)	0.48(5)

of HP sample. This means that for the HP sample with $x=0.50$ all the Fe atoms located in CuO_x chains have fivefold oxygen coordination, which is similar to the results of $\text{YSr}_2\text{Cu}_{2.7}\text{Fe}_{0.3}\text{O}_{7+y}$ prepared by high-pressure oxygen annealing.¹⁸ From the data listed in Table I, it can be found that for the AM sample with $x=0.50$ the sum of integrated intensities of doublets A and C is almost equal to that of doublet C in the spectrum of the HP sample, indicating that the integrated intensities of Fe located in CuO_x chains is not changed after the high-pressure synthesis. In the Mössbauer spectroscopy, site-integrated intensities are proportional to site occupancy N if we assume that the recoil-free fraction is same.³⁰ Thus, for the AM and HP samples, 76% of Fe content occupies Cu (1) sites in CuO_x chains and 24% of Fe content occupies Cu (2) sites in CuO_2 planes. The results of Mössbauer spectroscopy indicate that the high-pressure synthesis does not result in the migration of Fe from CuO_2 planes to CuO_x chains.

From Mössbauer spectra, it can also be determined that the Fe corresponding to doublets A and B have valence of +3 and the Fe associated with doublet C and D is Fe^{4+} species,^{18,29} indicating that the average valence of Fe ion in the HP samples is higher than that in the AM sample.

III. DISCUSSIONS

The perovskite structure of the Y123 compound has two copper sites Cu(1) in CuO_x chains and Cu(2) in CuO_2 planes. From the results of the neutron and Mössbauer spectra data,^{5,11,12,18,31} it was found that the Fe can occupy two Cu sites and Co only substitutes for Cu(1).^{18,32} Most of the previous studies on the Fe- or Co-doped Y123 system attempted to correlate the decrease of T_c with the magnetic pair-breaking effect because of magnetism of Fe^{3+} and Co^{3+} ions.^{8,33}

In recent years, however, the superconductivity was improved and discovered in $\text{YSr}_2\text{Cu}_{2.7}\text{Fe}_{0.3}\text{O}_{7+y}$,¹⁸ $\text{FeSr}_2\text{YCu}_2\text{O}_{7+y}$,¹⁹ and codoped $\text{CoSr}_2\text{Y}_{1-x}\text{Ca}_x\text{Cu}_2\text{O}_{7+y}$ compounds³⁴ synthesized under the high-pressure oxygen condition.

Why can the high-pressure oxygen synthesis and the high-pressure oxygen annealing enhance T_c of $\text{YSr}_2\text{Cu}_{2.7}\text{Fe}_{0.3}\text{O}_{7+y}$, $\text{FeSr}_2\text{YCu}_2\text{O}_{7+y}$, and codoped $\text{CoSr}_2\text{Y}_{1-x}\text{Ca}_x\text{Cu}_2\text{O}_{7+y}$ compounds? Three explanations were put forward to answer this question as follows. (1) The improvement of superconductivity in the $\text{YSr}_2\text{Cu}_{2.7}\text{Fe}_{0.3}\text{O}_{7+y}$ was attributed to the increases of oxygen content and the trigonal bipyramidal coordinated Fe at Cu (1) site in CuO_x chains due to high-pressure oxygen annealing.¹⁸ This explanation is supported by the results of XRD, measurements of oxygen content and Mössbauer effect analysis.¹⁸ (2) For the $\text{FeSr}_2\text{YCu}_2\text{O}_{7+y}$ superconductor prepared by calcining at 900 °C in air, subsequent annealing at 800 °C in flowing N_2 and then oxidizing at 350 °C in high-pressure oxygen of 195 atm, superconductivity is induced by both the ordering of Cu and Fe atoms in chains and the increase of oxygen content.^{19,20,26,28} (3) The occurrence of superconductivity in the $\text{CoSr}_2\text{Y}_{1-x}\text{Ca}_x\text{Cu}_2\text{O}_{7+y}$ system was attributed to the presence of the excess holes³⁴ due to the increase of oxygen content and the substitution of Ca^{2+} for Y^{3+} .

From our present work, it was found that the high-pressure synthesis not only increases oxygen content but also modifies the local structure on the atomic scale. For instance, in the Mössbauer spectra of the HP samples with lower Fe content of $x \leq 0.40$ the site B has singlet splitting, suggesting that oxygen environment about Fe(2) has higher symmetry. At the same time, Fe(1) in CuO_x chains has fivefold and sixfold oxygen coordination. These changes of the local structure are possibly conducive to the improvement of superconductivity.

In order to understand well the changes of the local structure, one can compare the Mössbauer spectrum of the HP sample with $x=0.5$ with that of its AM sample [see Figs. 12(1) and 12(2)]. It is found that the Mössbauer spectrum of the AM sample consists of three subspectra and that of the HP sample only consists of two subspectra. According to the assignments of Fe configuration, one can find that for the HP sample all the Fe(1) atoms in CuO_x chains have fivefold oxygen coordination (trigonal bipyramid).¹⁸ The fivefold oxygen coordination has been discussed in $\text{YSr}_2\text{Cu}_{2.7}\text{Fe}_{0.3}\text{O}_{7+y}$ superconductor synthesized by high-pressure oxygen annealing.¹⁸ It is possible that the trigonal bipyramidal coordinated Fe in the chains improve the coupling between the two adjacent CuO_2 planes¹⁸ and is favorable to charge transfer from CuO_x chains to CuO_2 planes. Therefore, the superconductivity in Fe-doped YBCO is improved after the high-pressure synthesis.

The results of Mössbauer effect indicate that for the sample with $x=0.50$ 20% of the whole Fe content is located in CuO_2 planes and Fe(2) is the Fe^{3+} species with magnetism. It is worth noting that the T_c of the HP sample with $x=0.5$ is enhanced up to 80 K, suggesting that the magnetic pairing-breaking effect is not obvious. Since the variation of oxygen content does not change the distribution of Fe between Cu (2) and Cu (1) sites¹⁸ and after the high-pressure synthesis the T_c of the HP samples with low Fe content can be increased up to that of pure YBCO, the decrease of T_c of Fe-doped YBCO is reasonably attributed to the hole fillings of Fe^{3+} and Fe^{4+} ions in CuO_x chains and CuO_2 planes, respectively.^{16,35} In Ref. 16, Terziev *et al.* found that in $\text{Y}_{1-z}\text{Ca}_z\text{Sr}_2\text{Cu}_{2.6}\text{Fe}_{0.4}\text{O}_{7+y}$ compound the addition of $x=0.1$ Ca increases T_c from 0 to 28 K. The same phenomenon was found by Smith *et al.* in the $\text{Y}_{1-z}\text{Ca}_z\text{Sr}_2\text{Cu}_{2.5}\text{Fe}_{0.5}\text{O}_{7+y}$ compound.¹⁷ Terziev *et al.*¹⁶ and Smith *et al.*¹⁷ determined the distribution of Fe between Cu(1) sites and Cu(2) sites and found that about 15% of Fe content is located in the CuO_2 planes for $\text{Y}_{0.9}\text{Ca}_{0.1}\text{Sr}_2\text{Cu}_{2.6}\text{Fe}_{0.4}\text{O}_{7+y}$ and

$\text{Y}_{0.9}\text{Ca}_{0.1}\text{Sr}_2\text{Cu}_{2.5}\text{Fe}_{0.5}\text{O}_{7+y}$ compounds. Moreover, in these two compounds the Fe(2) is Fe^{3+} species with high spin 5/2 which does not produce magnetic pair-breaking effect. Thus revivals of superconductivity in $\text{Y}_{0.9}\text{Ca}_{0.1}\text{Sr}_2\text{Cu}_{2.6}\text{Fe}_{0.4}\text{O}_{7+y}$ and $\text{Y}_{0.9}\text{Ca}_{0.1}\text{Sr}_2\text{Cu}_{2.5}\text{Fe}_{0.5}\text{O}_{7+y}$ compounds were reasonably attributed to the introduction of excess holes by the substitution of Ca^{2+} for Y^{3+} .^{16,17} In other words, the decrease of T_c in Fe-doped Y123 is caused by the hole fillings of Fe^{3+} and Fe^{4+} ions.^{16,35} This conclusion is well consistent with the results obtained by Faiz *et al.* using x-ray absorption spectroscopy to study Fe-doped YBCO.³⁵

Based on the above, it is speculated that for the AM samples with high Fe content of $x > 0.3$, the oxygen uptake in air only satisfies the charge balances and does not provide excess holes which participate in superconductivity. For the HP samples, excess holes were produced due to the high-pressure synthesis. Thus, the superconductivity in Fe-doped YBCO is improved in the HP samples.

One will ask why the Fe^{3+} ion with magnetism does not destroy the superconductivity in HP samples with high Fe content? By the magnetic measurements, it is found that the weak ferromagnetism and superconductivity coexist in the HP sample with $x=0.50$ by the formation of a spontaneous vortex phase (SVP).³⁶ Moreover, the SVP prevents ferromagnetism from destroying superconductivity.³⁶

IV. CONCLUSIONS

In this paper, the structure, oxygen content, superconductivity and Mössbauer spectroscopy measurements on $\text{Fe}_x\text{Cu}_{1-x}\text{Ba}_2\text{YCu}_2\text{O}_{7+y}$ superconductors synthesized by high pressure were systematically studied. On the one hand, the high-pressure synthesis led to the increase of the oxygen content and improvement of the superconductivity in the HP samples. On the other hand, the number of sixfold or fivefold oxygen coordinated Fe in the chains increases after the high-pressure synthesis, i.e., the high-pressure synthesis modifies the local structure on the atomic scale. Thus, it is suggested that the increases of oxygen content and the coordination number of Fe in the chains are the important factors for the improvement of superconductivity in the HP samples.

ACKNOWLEDGMENTS

This work was supported by the Ministry of Science and Technology of China (Grant No. G199064601) and the National Knowledge Innovation Program of Chinese Academy of Sciences (Grant No. GKJXC2-SW-W06-1).

*Electronic address: yhliu@ssc.iphyc.ac.cn

¹Gang Xiao, M. Z. Cieplak, A. Gavrin, F. H. Streitz, A. Bakhshai, and C. L. Chien, Phys. Rev. Lett. **60**, 1446 (1988).

²Y. Fukuzumi, K. Mizuhashi, K. Takenaka, and S. Uchida, Phys. Rev. Lett. **76**, 684 (1996).

³C. Bernhard, J. L. Tallon, C. Bucci, R. De Renzi, G. Guidi, G. V. M. Williams, and Ch. Niedermayer, Phys. Rev. Lett. **77**, 2304

(1996).

⁴S. A. Hoffman, M. A. Castro, G. C. Follis, and S. M. Durbin, Phys. Rev. B **49**, 12 170 (1994).

⁵B. D. Dunlap, J. D. Jorgensen, S. Sege, A. E. Dwight, J. L. Matykievicz, H. Lee, W. Peng, and C. W. Kimball, Physica C **158**, 397 (1989).

⁶M. G. Smith, R. D. Taylor, and H. Oesterreicher, J. Appl. Phys.

- 69**, 4894 (1991).
- ⁷I. Felner, D. Hechel, A. Rykov, and B. Raveau, *Phys. Rev. B* **49**, 686 (1994).
- ⁸J. M. Tarascon, P. Barboux, P. F. Miceli, L. H. Greene, G. W. Hull, M. Eibschutz, and S. A. Sunshine, *Phys. Rev. B* **37**, 7458 (1988).
- ⁹Y. Oda, H. Fujita, H. Toyoda, T. Kaneko, T. Kohara, I. Nakada, and K. Asayama, *Jpn. J. Appl. Phys., Part 2* **26**, L1660 (1987).
- ¹⁰C. Vaast, J. A. Hodges, P. Bonville, and A. Forget, *Phys. Rev. B* **56**, 7886 (1997).
- ¹¹I. Felner, U. Asaf, Y. Levi, and O. Millo, *Phys. Rev. B* **55**, R3374 (1997).
- ¹²E. B. Sonin and I. Felner, *Phys. Rev. B* **57**, R14 000 (1998).
- ¹³Y. Tokunaga, H. Kotegawa, K. Ishida, Y. Kitaoka, H. Takagiwa, and J. Akimitsu, *Phys. Rev. Lett.* **86**, 5767 (2001).
- ¹⁴C. Bernhard, J. L. Tallon, E. Brücher, and R. K. Kremer, *Phys. Rev. B* **61**, R14 960 (2000).
- ¹⁵T. Den and T. Kobayashi, *Physica C* **196**, 141 (1992).
- ¹⁶V. Terziev, R. Suryanarayanan, Mamidanna S. R. Rao, L. Ouhammou, and O. Gorochoy, *Phys. Rev. B* **48**, 13 037 (1993).
- ¹⁷M. G. Smith, J. Chan, and J. B. Goodenough, *Physica C* **208**, 412 (1993).
- ¹⁸F. Shi, W. J. Bresser, M. Zhang, Y. Wu, D. McDaniel, and P. Boolchand, *Phys. Rev. B* **54**, 6776 (1996).
- ¹⁹J. Shimoyama, K. Otszchi, T. Hinouchi, and K. Kishio, *Physica C* **341-348**, 563 (2000).
- ²⁰T. Mochiku, Y. Nakano, K. Oikawa, T. Kamiyama, H. Fujii, Y. Hata, J. Suzuki, I. Kakeya, K. Kadowaki, and K. Hirata, *Physica C* **400**, 43 (2003).
- ²¹Yinghao Liu, Guangcan Che, Keqiang Li, Hong Chen, Shunlian Jia, Weiwen Huang, and Zhongxian Zhao, *Physica C* **399**, 61 (2003).
- ²²Z. A. Ren, G. C. Che, Y. M. Ni, C. Dong, H. Che, S. L. Jia, and Z. X. Zhao, *Phys. Rev. B* **69**, 014507 (2004).
- ²³C. Dong, *J. Appl. Crystallogr.* **32**, 838 (1999).
- ²⁴J. D. Jorgensen, B. W. Veal, A. P. Paulikas, L. J. Nowicki, G. W. Crabtree, H. Claus, and W. K. Kwok, *Phys. Rev. B* **41**, 1863 (1990); W. K. Kwok, G. W. Crabtree, A. Umezawa, B. W. Veal, J. D. Jorgensen, S. K. Malik, L. J. Nowicki, A. P. Paulikas, and L. Nunez, *ibid.* **37**, 106 (1988).
- ²⁵B. Okai and M. Ohta, *Jpn. J. Appl. Phys., Part 2* **30**, L1378 (1991).
- ²⁶T. Mochiku, Y. Mihara, Y. Hata, Sh. Kamisawa, M. Furayama, J. Suzuki, K. Kadowaki, N. Metoki, H. Fujii, and K. Hirata, *J. Phys. Soc. Jpn.* **71**, 790 (2002).
- ²⁷E. H. Appenlan, L. R. Moss, A. M. Kinni, V. Gieser, A. Umezawa, G. W. Crabtree, and K. D. Karlson, *Inorg. Chem.* **26**, 3237 (1987).
- ²⁸T. Mochiku, Y. Mihara, Y. Hata, S. Kamisawa, J. Suzuki, K. Kadowaki, H. Fujii, and K. Hirata, *Physica C* **378-381**, 147 (2002).
- ²⁹M. G. Smith, R. D. Taylor, and J. D. Thompson, *Physica C* **208**, 91 (1993).
- ³⁰E. B. Saitovitch, R. B. Scorzelli, I. Souza Azevedo, and H. Micklitz, *Phys. Rev. B* **41**, 2103 (1990).
- ³¹A. M. Balagurov, G. M. Micronova, A. Pajaczowska, and H. Szymczak, *Physica C* **158**, 265 (1989).
- ³²P. F. Miceli, J. M. Tarascon, L. H. Greene, P. Barboux, F. J. Rotella, and J. D. Jorgensen, *Phys. Rev. B* **37**, 5932 (1988).
- ³³Q. Huang, R. J. Cava, A. Santoro, J. J. Krajewski, and W. F. Peck, *Physica C* **193**, 196 (1992).
- ³⁴Y. Morita, H. Yamauchi, and M. Karppinen, *Solid State Commun.* **127**, 493 (2003).
- ³⁵M. Faiz, X. Zhou, E. J. Moler, S. A. Kellar, Z. Hussain, N. M. Hamdan, and Kh. A. Ziq, *J. Electron Spectrosc. Relat. Phenom.* **103**, 707 (1999).
- ³⁶Y. H. Liu, G. C. Che, K. Q. Li, and Z. X. Zhao, *Supercond. Sci. Technol.* **17**, 1097 (2004).